Articles in PresS. Am J Physiol Endocrinol Metab (February 26, 2013). doi:10.1152/ajpendo.00596.2012

Title: **FGF23 is a novel regulator of intracellular calcium and cardiac contractility in addition to cardiac hypertrophy**

Authors: **Chad D. Touchberry[1], Troy M. Green[1], Vladimir Tchikrizov[1], Jaimee E. Mannix[1], Tiffany F. Mao[1], Brandon W. Carney[1], Magdy Girgis[5], Robert J. Vincent[5], Lori A. Wetmore[3], Buddhadeb Dawn[5], Lynda F. Bonewald[2], Jason R. Stubbs[4], and Michael J. Wacker[1]**

Affiliations: Muscle Biology Group, School of Medicine[1]; Bone Biology Group, School of Dentistry[2], University of Missouri-Kansas City, Kansas City, MO 64108. Department of Chemistry[3], William Jewell College, Liberty, MO 64068. The Kidney Institute[4] and the Division of Cardiovascular Diseases[5], University of Kansas Medical Center, Kansas City, KS 66160.

Corresponding Author:

Michael J. Wacker, PhD
School of Medicine
University of Missouri-Kansas City
2464 Charlotte Street
Kansas City, MO 64108
Email: wackerm@umkc.edu
Phone: 816-235-6069

Running Head: FGF23 alters cardiac contractility and induces hypertrophy

Key Words: Fibroblast Growth Factor 23, pathological cardiac hypertrophy, chronic kidney disease, Col4a3, FGFR, klotho

Abstract

Fibroblast growth factor 23 (FGF23) is a hormone primarily released by osteocytes that regulates phosphate and vitamin D metabolism. Recent observational studies in humans suggest that circulating FGF23 is independently associated with cardiac hypertrophy and increased mortality, but it is unknown if FGF23 can directly alter cardiac function. We found that FGF23 significantly increased cardiomyocyte cell size *in vitro*, the expression of gene markers of cardiac hypertrophy, and total protein content of cardiac muscle. In addition, *FGFR1* and *FGFR3* mRNA were the most abundantly expressed FGF receptors in cardiomyocytes and the co-receptor *α-Klotho* was expressed at very low levels. We tested an animal model of chronic kidney disease (*Col4a3*$^{-/-}$ mice) which has elevated serum FGF23. We found elevations in common hypertrophy gene markers in *Col4a3*$^{-/-}$ hearts compared to wild type, but did not observe changes in wall thickness or cell size by week 10. However, the *Col4a3*$^{-/-}$ hearts did show reduced fractional shortening (-17%) and ejection fraction (-11%). Acute exposure of primary cardiomyocytes to FGF23 resulted in elevated intracellular Ca^{2+} ($[Ca^{2+}]i$) (F/F_o +86%) which was blocked by verapamil pretreatment. FGF23 also increased ventricular muscle strip cardiac contractility (67%) which was inhibited by FGF receptor antagonism. We hypothesize that while FGF23 can acutely increase $[Ca^{2+}]i$, chronically this may lead to decreases in contractile function or stimulate cardiac hypertrophy as observed with other stress hormones. In conclusion, FGF23 is a novel bone-heart endocrine factor and may be an important mediator of cardiac Ca^{2+} regulation and contractile function during chronic kidney disease.

Introduction

Fibroblast growth factor 23 (FGF23) is a hormone primarily released by osteocytes (2, 4, 14, 38), that functions to regulate phosphate and vitamin D homeostasis through direct actions on the kidney and parathyroid (2). While an endocrine axis has been established between bone and kidney, a new paradigm is emerging in which FGF23 could be important in establishing an endocrine axis between bone and heart. Circulating levels of FGF23 are markedly elevated 100 - 1000 fold in patients with chronic kidney disease (CKD) (24, 31) and are independently associated with cardiovascular morbidity and mortality (8, 22, 26, 34, 35, 48, 52). Specifically, an association between left ventricular hypertrophy and serum FGF23 levels has been established in chronic kidney disease (CKD) patients (20, 36, 52).

Nevertheless, despite strong associations between FGF23 and adverse outcomes, it remains relatively unknown if FGF23 is simply a marker of cardiac disease risk or a direct mediator of cardiac pathology and cardiac performance. Only one study to date has analyzed the direct effects of FGF23 on the heart both *in vitro* and *in vivo* (13). This important work by Faul et al. (13) shows that FGF23 can directly induce hypertrophy in isolated neonatal cardiomyocytes as well as with intramyocardial FGF23 injections. They also demonstrated that a FGF receptor (FGFR) antagonist reduced the left ventricular hypertrophy in a 5/6 nephrectomy rat model of CKD. These findings are significant in that FGF23 may be an important player in directly inducing cardiac hypertrophy during chronic kidney disease.

Moving forward, our lab has explored and addressed crucial questions that require answers such as can the hypertrophic effects of FGF23 also be replicated in adult cardiomyocytes and observed in another animal model of chronic kidney disease ($Col4a3^{-/-}$) which has elevated serum FGF23? Secondly, can FGF23 directly alter intracellular Ca^{2+}

($[Ca^{2+}]i$) and cardiac contractility? Previous studies have found a clinical association between FGF23 and left ventricular mass (22, 35, 52), as well as declines in cardiac performance as measured by reduction in ejection fraction (19). However, to date no investigation has determined if FGF23 can alter cardiac function independent of changes in cardiac hypertrophy. Determining what direct effects FGF23 may have on the heart will not only reveal how FGF23 may alter cardiac function on a beat to beat basis but also will yield insights into how this hormone may induce chronic pathologies such as hypertrophy or heart failure.

Material and Methods

Materials

Recombinant mouse FGF23 was purchased from R&D Systems (Minneapolis, MN). The FGFR1 inhibitor, PD166866 was purchased from EMD biosciences (San Diego, CA). Organ baths, stimulating electrodes, and LabChart 6 software were obtained from AD Instruments (Colorado Springs, CO). The stimulation unit (SD9) was purchased from Grass Technologies (Quincy, MA). Hanks' balanced salt solution and Flou-4 AM were obtained from Invitrogen (Carlsbad, CA). Enzymes for cardiomyocyte isolation were obtained from Worthington (Lakewood, NJ). Total RNA isolation kits were purchased from IBI scientific (Peosta, IA) and the real-time reverse transcriptase polymerase chain reaction (RT-PCR) was performed using a TaqMan RNA-to CT 1-step kit from ABI (Carlsbad, CA). β-Tubulin and phospho-ERK1/2 antibodies were purchased from Cell Signaling (Danvers, MA). NCX1 primary antibodies were purchased from Swant (Marly, Switzerland). Claycombs medium and fetal bovine serum was purchased from Sigma-Aldrich (St. Louis, MO). All remaining reagents were purchased from Fisher Scientific (Pittsburgh, PA).

Experimental Animals

Twelve-week-old wild type (WT) male CD1 mice (Harlan Laboratories; Madison, WI) were used in experiments using exogenous FGF23. In addition, male and female 10-week-old *Col4a3*$^{-/-}$ mice (background SV129) and age/liter matched WT mice were also used in this study. The *Col4a3*$^{-/-}$ mice are a model of human autosomal-recessive Alport syndrome and have elevated serum levels of FGF23 up to >5000 pg/ml by 12 weeks (46). The *Col4a3*$^{-/-}$ mice develop non-hypertensive progressive renal fibrosis (17, 18). By 12 weeks *Col4a3*$^{-/-}$ mice present with significant elevations in serum phosphorus, parathyroid hormone, blood urea nitrogen, and creatine when compared to WT mice (46). In addition, at week 12, *Col4a3*$^{-/-}$ mice have significantly reduced serum calcium and $1,25(OH)_2D$ (46). All mice were housed in a temperature-controlled (22 ± 2 °C) room with a 12-h:12-h light/dark cycle. Animals were fed *ad libitum*. All protocols were approved by the Animal Care and Use Committee of the University Missouri-Kansas City School of Medicine and the University of Kansas Medical Center.

HL-1 Cell Culture

HL-1 cardiomyocytes were plated (5000/cm^2) in flasks pre-coated with 0.00125% fibronectin and 0.02% gelatin. Cells were cultured for 24 h in Claycomb's media (supplemented with 10% FBS, 2 mM L-glutamine, 0.1 mM norepinephrine, 0.3 mM ascorbic acid, 100 units/ml penicillin, and 100 mg/ml streptomycin as previously described (50, 51). Prior to experiments, cells were rendered quiescent in a minimal media (0.5% FBS, 2 mM L-glutamine, penicillin/streptomycin; without norepinephrine) for 48 h prior to treatment. Cells were treated with vehicle, FGF23, FGF23 + PD166866 (50 nM) for 48 h prior to analysis. Cells were collected and analyzed for changes in cells size by flow cytometry using FACSCalibur (FSC).

Isolation of Primary Cardiac Myocytes

Following cervical dislocation the heart was rapidly excised, extraneous tissue was removed and the aorta was cannulated under a dissection scope. Cardiomyocytes were isolated in a standard manner utilizing retrograde perfusion via a proprietary procedure developed in our laboratory with Worthington Biochemical Corporation (Lakewood, NJ). Briefly, hearts were retrograde perfused through the aorta using a Langendorff perfusion apparatus with Ca^{2+}-free perfusion buffer (3ml/min) for 4 min, then switched to a digestion buffer containing collagenase II (18,000 units), Papain (20 units) and DNase (2000 units) for 8-10 min at 37°C. The heart was removed from perfusion, cut into pieces and pipetted gently to disperse cells in suspension. Calcium tolerant myocytes were then plated into dishes previously coated with 10 μg/ml laminin and kept in L-15 medium with blebbistatin (25 μM) (27).

Gene Expression

Total RNA from isolated cardiomyocytes, FGF23 or vehicle treated cardiac tissue cultures, and *Col4a3*$^{-/-}$ and WT mice were extracted and real-time RT-PCR was performed. Gene expression from tissue culture was normalized ($2^{-\Delta\Delta CT}$ analysis) to β-actin (55). Gene expression for isolated cardiac myocytes was performed using $2^{-\Delta CT}$ analysis against β-actin and then normalized to *α-Klotho* expression. For WT and *Col4a3*$^{-/-}$ mice gene expression, $2^{-\Delta CT}$ analysis was performed using β-actin as a standard and then averages of each gene of the WT mice were calculated. Each individual animal was then normalized to the average of the WTs. β-actin was chosen as a housekeeping gene as FGF23 treatment and *Col4a3*$^{-/-}$ mice models had minimal changes in gene expression compared to vehicle treated and WT mice respectively. GAPDH comparisons also yielded similar results as that with β-actin.

Tissue Culture

CD1 mouse ventricular tissue strips were isolated from mouse hearts and used for the tissue culture experiments. Hearts were quickly excised and placed into an ice-cold cardioprotective medium that included the addition of 2,3-butanedione monoxime (30 mM) as previously described (50). Tissue cultures were treated with vehicle, FGF23, or FGF23 + PD166866 (50 nM).

Total Protein & Western Blot

Clamp-frozen ventricular tissues were weighed and homogenized in a 12:1 (volume/weight) ratio of ice-cold cell extraction buffer (Invitrogen) as previously described (56). Total protein concentration of the samples was determined by use of the micro-bicinchoninic acid protein assay (Pierce Chemical) and then normalized to tissue weight (μg/mg). Protein samples (20-50 μg) were run on 4-20% SDS-PAGE gels and western blots were performed using standard techniques. Because downstream changes in the signaling pathway are reliant on a net increase in ERK phosphorylation and total ERK protein expression is unlikely to change over 15 minutes, p-ERK blots were normalized to β-tubulin as a loading control. Whole heart lysates from WT and *Col4a3*$^{-/-}$ mice were used for analysis of NCX1 via western blotting and were normalized to β-tubulin.

Echocardiogragphy on Col4a3$^{-/-}$ *mice*

Mice were weighed and anesthetized with isoflurane inhalation (3% for induction, 1% for maintenance). The anterior chest was shaved and the mice were placed on a heating pad in the left lateral decubitus position. A rectal temperature probe was placed to ensure that the body temperature remained at 37.0°C during the study. Left ventricular (LV) structure and function were assessed by previously validated two-dimensional, M-mode, and Doppler echocardiographic techniques (9, 61). Echocardiographic images were obtained using a Philips

HDI 5000 SonoCT ultrasound system equipped with a 12-5 MHz phased-array probe fitted with a 0.3 cm standoff and a 15-7 MHz broadband linear probe. Digital images were analyzed off-line according to modified American Society for Echocardiography standards (42) using the ProSolv image analysis software (version 3.5, Problem Solving Concepts). LV end-diastolic (LVEDD) and end-systolic diameters (LVESD) and anterior and posterior wall thickness in diastole were measured from M-mode tracings obtained at the midpapillary level (41). LV ejection fraction was derived from M-mode parameters. LV mass was estimated from the M-mode data and LV end-diastolic (LVEDV) and end-systolic (LVESV) volumes were calculated using the Teichholz formula (49). Analysis of data was performed by an investigator blinded to the treatment assigned.

Histology

Hearts were removed and fixed in 4% paraformaldehyde for 24 h, embedded in paraffin and sectioned (5 μm). Sections were deparaffinized and stained with wheat germ agglutinin (WGA) or picrosirius red. Measurements of the cross-sectional area (n>250 cells from both male and female animals) were obtained from images using Slidebook software (Intelligent Imaging Innovations Inc., Denver, CO)].

Ca^{2+} Imaging

Imaging during FGF23 perfusion was conducted as reported previously (50, 51, 57). Briefly, cells were loaded at room temperature with the fluorescent Ca^{2+} indicator Fluo-4-AM (2 μM) for 20 min. Cells were washed three times in HBSS and allowed to de-esterify for 10 min at room temperature. Intracellular Ca^{2+} levels were measured with an inverted microscope with fluorescent imaging capabilities [Olympus IX51, Olympus, Melville, NY; Hamamatsu Orca-ERGA CCD camera (Hamamatsu, Bridgewater, NJ); Semrock Bright Line filter set (Semrock,

Rochester, NY), EXFO X-cite metal halide light source (EXFO, Mississauga, ON, Canada), and Slidebook ratiometric software (Intelligent Imaging Innovations Inc., Denver, CO)]. Diluted FGF23 (18,000 pg/ml) was carefully perfused to the plates at a rate of 0.3 ml/min. In these experiments, the five treatment conditions (1: vehicle, 2: FGF23 alone, 3: PD166866 (50 nM) + FGF23, 4: FGF23 in the presence of 0 mM extracellular Ca^{2+}, 5: Verapamil (10 μM + FGF23) were tested 5 times which totaled 6-10 cardiomyocytes from a given animal from 3-5 different animals. The fluorescent changes from each cell were averaged and the data were grouped by animal and then used for data analysis. All data are presented as the peak increase in fluorescence (F) after FGF23 application divided by the initial fluorescence before FGF23 application (F_0). A F/F_0 of 1 indicates no change in fluorescence from the baseline. Cells were tested for viability with KCl (80 mM) at the end of each experiment, and were only included in the data set if the response to KCl was greater than a 50% increase from baseline fluorescence.

Cardiac Contractility Measurements

CD1 mice were euthanized by cervical dislocation. The mouse hearts used for the muscle strip experiments were quickly excised and placed into an ice-cold cardioprotective Ringer's solution (with Ca^{2+}) that included the addition of 2,3-butanedione monoxime (30 mM) and insulin (10 IU/liter) for 30 min as described previously (50). Briefly, left ventricular muscle strips were prepared (1–2 mm wide by 6–8 mm long) in the cardioprotective solution. The strips were tied on the proximal and distal ends with a silk thread. The muscle strips were then rinsed three times (5 min each) in Ringer's (with Ca^{2+}, pH, 7.4) to remove the 2,3-butanedione monoxime. The muscle strips were hung vertically and attached to force transducer, between bipolar platinum stimulating electrodes suspended in 25-ml glass tissue chambers and bubbled under 100% O_2 . Heart muscles were stretched to the length of maximum force development in

Ringer's solution (pH, 7.4, without 2,3-butanedione monoxime) and stimulated with pulses of 1 Hz, for 5 ms. The stimulation voltage was set 20% above threshold and the muscles in the chamber were superfused with Ringer's solution (with Ca^{2+}, pH, 7.4). Muscles were allowed to stabilize for 90 min prior to experimentation and provided with fresh media changes every 30 min. Muscles were paced at 1 Hz to obtain a stable baseline and were treated with either vehicle or FGF23. The contractile data were recorded and analyzed on the LabChart 6 software. Waveform changes were analyzed in the segments corresponding to peak isometric tension (mN). Slope (mN/s) was analyzed by taking the average slope from 10 to 20 ms after the start of the peak. Area (mN×s) was calculated using the region from 10 to 90% of the peak. τ (s) was fitted at the baseline using data from 95 to 0% of peak. Strip experiments were normalized within each condition to baseline levels of contractility and presented as a relative change from baseline contraction data.

Statistical Analysis

All graphs were made and statistical procedures were performed using GraphPad Prism 5.0. Data are presented as means ± S.E. Data were compared using either a paired *t* test or a one-way analysis of variance, and significance was set at the $p \leq 0.05$ level. When necessary, the one-way analysis of variance was followed with appropriate post hoc tests. A Bonferroni post hoc adjustment was used to correct for 2-3 comparisons to avoid type I error. In cases where we made >3 comparisons we utilized a Tukey Post hoc adjustment to avoid type II error. FACSCalibur data was analyzed using FlowJo® Version 8.8.6 probability binning population comparison software (Tree Star, Inc.) using a modified Cox Chi Squared Test (T(X)). A value $T(X) > 4$ implies that the two distributions are different with a $p < 0.01$ (99% confidence).

Results

Markers of Cardiac Hypertrophy with exogenous FGF23

We began this series of studies by testing the hypothesis that FGF23 directly induces hypertrophy in cardiomyocytes. Flow cytometry revealed a concentration dependent increase in HL-1 cell-surface area of cardiomyocytes exposed to FGF23 ($T(X)=63$, $p<0.05$; Fig. 1A and B). Twenty-four h exposure of ventricular muscle strips to FGF23 (900 pg/ml) resulted in increased expression of EGR1, atrial natriuretic peptide (ANP) and brain natriuretic peptide (BNP) (Fig. 2A; $p < 0.05$). In addition, 48 h exposure to FGF23 increased gene expression of β-myosin heavy chain (β–MHC) and skeletal muscle α–actin (SkAct) (Fig. 2A; $p < 0.05$). No statistically significant changes were noted for c-Myc, c-Fos, or c-Jun following FGF23 treatment. It is well known that FGFR signaling in the kidney involves the activation of the MAPK cascade, particularly ERK (58). In cardiomyocytes, ERK phosphorylation is known to induce the early growth response 1 (EGR1) transcription factor, as well as increase fetal gene expression associated with pathological hypertrophy (33). ERK phosphorylation in isolated cardiac muscle strips was significantly increased 15 min after treatment with FGF23 when compared with vehicle treated strips (Fig. 2B; $p < 0.05$). In addition, FGF23 increased protein synthesis 8% (Fig. 2C; $p < 0.05$), and this increase was inhibited by the pre-addition of PD166866. This data suggests that changes in cell size are FGFR mediated and are not simply due to swelling.

FGFR and α-Klotho Gene Expression

We quantified the expression levels of FGFRs and *α-Klotho* in isolated cardiomyocytes (Fig.3A). The delta cycle threshold (dCT) values were calculated using *β-actin* as the reference gene and 2^{-dCT} calculations were performed. The order of expression from highest to lowest was *FGFR3, FGFR1, FGFR4, FGFR2,* and *α-Klotho*. For ease and clarity of data presentation, we

calculated the relative expression of each FGF receptor by comparing it to *α-Klotho* as shown in Fig. 3B. Statistical analysis was not conducted on this data since it was transformed and normalized to the lowest expressed gene. Statistical analysis was conducted on the raw dCT values. *FGFR3*, *FGFR1,* and *FGFR4* were significantly higher when compared to *α-Klotho* ($p < 0.05$). FGFR3 and FGFR1 did not statistically differ from one another ($p > 0.05$) but both were statistically higher than *FGFR4* and *FGFR2* ($p < 0.05$). *FGFR4* and *FGFR2* did not differ from one another ($p > 0.05$). Similar expression results were confirmed using *GAPDH* as the housekeeping gene.

Col4a3-/- Mice

Since we observed hypertrophic signaling occurring with exposure to FGF23, we analyzed ventricular heart tissue from 10 week old *Col4a3*$^{-/-}$ mice for markers of pathological hypertrophy. The *Col4a3*$^{-/-}$ mouse is a model of human Alport syndrome in which there is progression of CKD and therefore has elevated levels of FGF23 starting at week 6 (46). We observed increases in ANP, βMHC and SkAct in *Col4a3*$^{-/-}$ hearts when compared to hearts of their WT littermates (Fig. 4A; $p < 0.05$). Interestingly, we did not see gross morphological evidence of hypertrophy in the *Col4a3*$^{-/-}$ mice. There were no changes in anterior or posterior wall thickness when compared to WT controls as measured by echocardiography (Fig. 4B; $p > 0.05$). We did not detect an increase in heart size by estimates in LV mass from the echocardiogram, or by comparing heart weights to tibia length (HW/TL) (Fig. 4C; $p > 0.05$). In addition, the average cardiomyocyte cross-sectional area based on the histological analysis from both male and female mice were similar in *Col4a3*$^{-/-}$ and WT hearts (Fig. 4D and E). A randomly selected subsample of cross-sections were stained with picrosirius red and we did not observe any differences in fibrosis between WT and *Col4a3*$^{-/-}$ mice (mean % fibrosis of heart

sections = 0.46% vs 0.49% respectively; n=2). Representative M-mode tracings from echocardiography are shown in Fig. 5A. *Col4a3*$^{-/-}$ mice did exhibit declines in left ventricular function as determined by reductions in both fractional shortening (FS) and ejection fraction (EF) (-17% and -11% respectively; Fig. 5B; $p < 0.05$). Because there appeared to be a decrease in contractile function without hypertrophy, we hypothesized there may be Ca^{2+}-handling issues and therefore we tested 3 major Ca^{2+}-handling genes. Interestingly, *Col4a3*$^{-/-}$ mice hearts showed a significant up regulation of the Na^{+}/Ca^{2+} exchanger 1 (*NCX1*) mRNA (1.76 fold + 0.33, $p < 0.05$; n=5), however there was not a significant increase in NCX1 protein expression (1.15 + 0.09 vs 1.40 + 0.15, $p > 0.05$; n=6-7) over WT. In addition, there were no significant increases in calsequestrin (*Cal*) (1.39 fold + 0.28, $p > 0.05$; n=5) and sarcoplasmic/endoplasmic reticulum Ca^{2+}-ATPase (*SERCA*) (1.02 fold + 0.04, $p > 0.05$; n=5) mRNA expression in the *Col4a3*$^{-/-}$ mice hearts.

Ca^{2+} Imaging of Primary Cardiomyocytes

To determine if FGF23 can modulate the levels of $[Ca^{2+}]i$, we recorded the Ca^{2+} responses in primary cardiomyocytes with the fluorescent Ca^{2+} indicator Fluo-4 AM. Fig. 6A and B display a representative response of a cardiomyocyte to FGF23 (18,000 pg/ml). The myocyte displayed a spontaneous Ca^{2+} oscillation prior to treatment, and after FGF23 had a large and transient increase in $[Ca^{2+}]i$. FGF23 increased F/F_o by 86% on average in comparison to vehicle (Fig. 6C; $p < 0.05$). We were able to prevent these increases in $[Ca^{2+}]i$ by pretreating cells with PD166866 (Fig. 6C; $p < 0.05$). In addition, we were able to eliminate the increases in $[Ca^{2+}]i$ by eliminating extracellular Ca^{2+} and upon pre-treatment of the cells with the L-type voltage gated Ca^{2+} channel antagonist verapamil (10 μM) (Fig. 6D; $p < 0.05$). The average time for a peak response to perfused FGF23 was 186.6 $\pm$ 6.6 s. The average time for a peak response to perfused

KCl was 68.8 ± 5.6 s, and the average F/F_o response to KCl was 3.17 ± 0.41. The dead-space time of our perfusion system in these experiments was ~45 s. To test if prolonged exposure to FGF23 induced an increase in resting levels of Ca^{2+}, we loaded primary cardiomyocytes with the ratiometric fluorescent Ca^{2+} indicator Fura-2-AM. Cardiomyocytes treated with FGF23 for 2 h increased $[Ca^{2+}]i$ by 25% ($p < 0.05$; data not shown).

Contractility

Since FGF23 acutely increased $[Ca^{2+}]i$ we explored the effect of exogenous FGF23 in cardiac muscle contractility. We compared the contractile responses elicited by increasing concentrations of FGF23 compared to vehicle. Peak changes in contractility were noted between 15-20 min following FGF23 treatment. Fig. 7A displays raw tracings of paced ventricular muscle strips following treatment with vehicle and FGF23 (9000 pg/ml). Increasing concentrations of FGF23 (900 and 9000 pg/ml) increased isometric force, when compared with vehicle (Fig. 7B; $p < 0.05$). We analyzed the effects of FGF23 on specific characteristics of each contractile waveform. FGF23 (900 and 9000 pg/ml) increased the slope of contraction (Fig. 7C; $p < 0.05$), and the overall area (Fig. 7C; $p < 0.05$) of the contractile waveform (i.e. the integral/impulse) when compared with vehicle. FGF23, however, had no effect on τ, the time constant of decay (rate of relaxation), when compared to vehicle (Fig. 7C). To test if the changes in contractility were receptor mediated, we repeated a series of experiments with PD166866 (50 nM) which eliminated the increases in isometric tension, slope and overall area induced by FGF23 (Fig. 7D; $p < 0.05$). In addition, FGF23 and PD166866 had no effect on τ.

Discussion

There have been several recent clinical reports suggesting that FGF23 may alter heart function, particularly during CKD (15, 21, 22, 35). However, there have been very few studies

that have attempted to address the direct effects of FGF23 on the myocardium. Therefore, we sought to determine what alterations in cardiac function would occur during exposure to FGF23. The major findings of this study are as follows: 1) Exposure to FGF23 causes a dose dependent increase in cell size, as well as increased protein synthesis and expression of common hypertrophy markers; 2) the *Col4a3*$^{-/-}$ mouse model of CKD which is known to have elevated FGF23 demonstrates increased gene expression of markers of pathological hypertrophy but does not show increase in cardiomyocyte size or ventricular wall thickness; 3) *Col4a3*$^{-/-}$ mice have alterations in contractile function that appear to precede the potential development of pathological hypertrophy; 4) Acute exposure to FGF23 increases $[Ca^{2+}]i$ in adult ventricular myocytes; and 5) Acute FGF23 exposure alters cardiac contractility by increasing force, rate of force development, and the area under the curve (integral).

Hypertrophy

The normal level of FGF23 in the plasma in healthy patients is 13.3+19.0 pg/ml; however in CKD plasma FGF23 levels can rise 100-1000 fold higher than patients with normal renal function (25). In patients with CKD, these elevated serum levels of FGF23 have been clinically associated with increased left ventricular mass, and increased risk of left-ventricular hypertrophy (20, 35, 52). Moreover, FGF23 levels have been shown to predict outcomes in patients with systolic heart failure (39). However, despite these strong clinical associations, there has been only a single basic science study to date to show that FGF23 directly induces a hypertrophic phenotype in the heart (13). Therefore we determined if the hypertrophic effects of FGF23 could also be replicated in adult cardiomyocytes *in vitro* and whether hypertrophy is present in another animal model of chronic kidney disease (*Col4a3*$^{-/-}$) which has elevated serum FGF23.

In order to investigate the effects of FGF23 on hypertrophy, we first performed concentration-response experiments analyzing changes in cell size with HL-1 cardiomyocytes. We utilized concentrations of 90, 900, and 9000 pg/ml as that represents an approximate baseline level (in WT mice) and then 10 fold and 100 fold higher concentrations which would be expected during CKD. HL-1 cardiomyocytes were utilized as they: maintain phenotypic characteristics of adult myocytes (7), have been previously used in models of cardiac hypertrophy (5, 6, 30), do not contain fibroblasts, and can be used in large population numbers over extended periods of time to more accurately detect changes in cell size. Similar to Faul et al. (13) who used neonatal cardiomyocytes our data show that FGF23 induced HL-1 cell growth up to 24% in a concentration dependent manner. To validate that FGF23 could have a direct effect on cardiac tissue; we analyzed early growth response genes and fetal genes associated with pathological cardiac hypertrophy in ventricular muscle strips. Similar to previous reports (13, 53) we were unable to induce EGR1 expression 1 h following FGF23 exposure (data not shown); however, we report that FGF23 can induce EGR1 expression in cardiac tissue 24 h following administration. The expression of c-Myc (a mediator of growth signaling in cardiomyocytes), did not reach statistical significance despite increasing over 2 fold following treatment with FGF23. In addition, FGF23 treatment also resulted in the elevated expression of BNP, ANP, β-MHC, and SkAct, which are well known markers of cardiac hypertrophy. Specifically, there have been significant correlations between elevated FGF23 and elevated BNP plasma levels in patients with left ventricular hypertrophy (19, 43). BNP in particular is used as a diagnostic indicator for heart failure (12), suggesting that FGF23 may directly promote the progression of heart failure.

Previous research in non-cardiac tissue has shown that FGF23 is a potent inducer of ERK phosphorylation and subsequent EGR1 expression (1, 53, 58). In cardiac muscle strips treated

with FGF23, we noted a pERK response within 15 min of treatment. Interestingly, it has been previously reported that FGF23 did not increase cardiac expression of pERK at 30 and 60 minutes following exposure in neonatal cardiomyocytes (13). However, these authors did show that the ERK inhibitor U0126 was able to attenuate increases in FGF23 induced cell size (13). These differences with our findings for pERK may be due to differences in age (neonatal vs. adult), the tissue type (isolated myocytes vs. whole tissue), or the timing of the measurements in these studies.

Lastly, we applied exogenous FGF23 to cultured adult ventricular muscle strips and measured changes in total protein content. FGF23 increased protein synthesis following 48 h of treatment and this effect was also dependent on FGFR activation, as it was eliminated by pre-treatment with PD166866. Taken together, our data lend strength to the hypothesis that FGF23 can directly induce cardiac hypertrophy.

FGFRs and α-Klotho

It is currently unknown which receptors are necessary for FGF23 to exert its effects on the heart. FGF23 is known to bind FGFR1-FGFR4 with varying degrees of affinity (59, 60), and previous reports using end point RT-PCR and immunohistochemistry in neonatal cardiomyocytes and adult hearts have shown that FGFR1-4 are present (13, 23). Our data now extend these findings by using real-time RT-PCR to quantitate relative expression levels in isolated primary cardiomyocytes which showed that FGFR3 and FGFR1 are the most abundantly expressed. Since we were able to block the acute and chronic effects FGF23 with PD166866, a selective inhibitor of FGFR1 at 50 nM (37), and FGFR1 is abundantly expressed, it seems likely that FGFR1 is an important mediator of FGF23 cell signaling in the myocycardium.

FGF23 is thought to have a high binding affinity for FGFR1-α-Klotho complexes in other tissues like the kidney and parathyroid. In contrast to previous studies (13, 29, 47, 53), we have detected *α-Klotho* expression in the heart. Our ability to detect *α-Klotho* may be attributed to the increased sensitivity of the one-step real-time RT-PCR procedure (54). However, given that we found *α-Klotho* to be ~3750 fold lower in expression than our highest expressed gene, FGFR3, we support the hypothesis that α-Klotho likely plays a limited role in FGF23 signaling in cardiomyocytes (13). Moreover, it is possible that other FGFRs in addition to FGFR1 may be involved in FGF23 mediated actions on cardiomyocytes. Previous studies have suggested that FGFR1, FGFR3 and FGFR4 can act in concert to mediate FGF23 effects in the kidney (32). It has also been suggested that in the absence of α-Klotho, FGF23 has a high affinity for FGFR4 (23, 60) and may mediate effects on the heart (13). However, we would hypothesize that FGFR4 as well as FGFR2 may play limited roles due to their lower expression levels. Taken together, our data lend support to the hypothesis that FGF23 signaling in the heart may be independent of α-Klotho expression, and suggests that FGFR1 and FGFR3 may be critical to signaling in the heart. Nevertheless, a more thorough inquiry into exact mechanisms responsible for FGFR cardiac signaling awaits further investigation.

Evidence of cardiac dysfunction in Col4a3$^{-/-}$ mice

It has recently been shown that the 5/6 nephrectomized rat model of CKD develops left ventricular hypertrophy that was significantly attenuated with the FGFR antagonist PD173074 (13). Interestingly, another study found that a FGF23 neutralizing antibody did not reduce the hypertrophy in this animal model (44). Therefore, we were interested in exploring if a different model of CKD with elevated FGF23 could develop cardiac hypertrophy. The *Col4a3$^{-/-}$* mouse is a model of autosomal-recessive Alport syndrome. This mouse model is non-hypertensive and has a progressive increase in the serum levels of FGF23 that precedes elevations of traditional

markers of renal function (17, 18). From weeks 4 - 6 FGF23 levels increase from ~130 to ~260 pg/ml respectively. However, serum FGF23 levels increase exponentially from weeks 8 to 12 (440 to 5400 pg/ml respectively) (46). Therefore, we used *Col4a3*$^{-/-}$ mice to explore the connection between elevated serum FGF23 and cardiac hypertrophy. Similar to the 5/6 nephrectomized mice (13, 44), *Col4a3*$^{-/-}$ mice presented with increased gene expression markers of hypertrophy (ANP, SkAct, and βMHC); however we noted no changes in anterior/posterior wall thickness, nor increased cardiac mass by echocardiography or necropsy. Furthermore, there was no increase in average cardiomyocyte size based on histological analysis. The *Col4a3*$^{-/-}$ mouse model has significantly increased rates of mortality beginning at 10 weeks which prevented further characterization of these animals. We postulate that given additional time, these mice may have also demonstrated significant increases in cell size given that the hypertrophic gene markers were increased at 10 weeks.

While we did not observe hypertrophy, there were significant decreases in the contractile parameters (fractional shortening and ejection fraction). In the 5/6 nephrectomized animals, Faul et al. (13) reported declines in ejection fraction (although it did not reach statistical significance) which was observed concurrent with increases in hypertrophy. This decrease in ejection fraction was eliminated by a FGFR antagonist (13). Interestingly, the changes in contractility in the *Col4a3*$^{-/-}$ mice in our study occurred without significant hypertrophy or fibrosis and occurred in a CKD animal model that does not demonstrate chronic hypertension. The *Col4a3*$^{-/-}$ mouse model may thus provide an interesting tool for studying cardiac effects of FGF23. Differences in cardiac function between animal models with high FGF23 need to continue to be explored to fully elucidate cardiac effects of FGF23 *in vivo* during CKD.

The contractile deficits we observed in the animal model led us to explore if FGF23 is altering Ca^{2+} handling genes or directly altering Ca^{2+} levels. We first explored Ca^{2+} handling genes that are known to increase during heart failure. The *Col4a3*$^{-/-}$ mouse had a significant upregulation of *NCX1* mRNA but not *SERCA* or *Cal*. Interestingly, we did not observe a significant increase in NCX1 protein expression in *Col4a3*$^{-/-}$ mice when compared to WT. Because the NCX1 is an important regulator of $[Ca^{2+}]i$ in cardiomyocytes and is increased during cardiac hypertrophy (28, 40) future studies concerning the effects of FGF23 on the myocardium may be warranted.

Intracellular Ca^{2+}

Next, we wanted to explore if FGF23 could be directly altering $[Ca^{2+}]i$. Acute exposure of primary cardiomyocytes to FGF23 significantly increased $[Ca^{2+}]i$ and we were able to eliminate this increase via pretreatment with PD166866. Removing extracellular Ca^{2+} also abolished the FGF23 evoked increase in $[Ca^{2+}]i$, suggesting that FGF23 likely opens a Ca^{2+} channel on the cellular membrane of cardiomyoyctes to augment contraction, rather than altering release of Ca^{2+} from internal stores. To test this hypothesis, we pre-treated cardiomyoctyes with the L-type Ca^{2+} channel blocker, Verapamil. Pre-treatment with Verapamil also completely inhibited Ca^{2+} entry, suggesting FGF23 can effect L-type gating. Furthermore, prolonged exposure to FGF23 resulted in a 25% increase in basal levels of Ca^{2+}, suggesting that over time FGF23 may lead to Ca^{2+} overload. Increased basal levels of Ca^{2+} have been linked to remodeling and hypertrophy of the heart (3, 11, 16). Thus $[Ca^{2+}]i$ may be a critical link between elevated FGF23, acute alterations in cardiac function, long term remodeling, hypertrophy and ultimately heart failure.

Cardiac Contractility

Lastly, to determine the acute effects of this elevated $[Ca^{2+}]i$ we explored the effects of exogenous FGF23 on isolated ventricular muscle contractility. We hypothesized that the increases in $[Ca^{2+}]i$ were large enough to acutely improve cardiac contractility. We have shown for the first time that FGF23 significantly increases isometric tension, slope, and the area of contraction in isolated cardiac muscle. During cardiac excitation contraction coupling, force is generated on a beat-to-beat basis by a 10-fold increase in cytosolic Ca^{2+} by process known as Ca^{2+}-induced Ca^{2+} release (CICR). As a cardiac myocyte depolarizes, $[Ca^{2+}]i$ begins to accumulate principally from the opening of L-type voltage gated Ca^{2+} channels, which triggers CICR from RyR2 to drive muscle contraction. Therefore, $[Ca^{2+}]i$ increases are tightly coupled to increased cardiac contractility. Our data showing an increase not only the in the magnitude, but also in the slope and area suggest that FGF23 may alter the CICR mechanism, allowing for greater $[Ca^{2+}]i$, thus promoting faster and more powerful contractions. Our changes in tension, slope and area lend strength to our data showing that FGF23 promotes Ca^{2+}entry via L-Type Ca^{2+} channels. During relaxation, a return to Ca^{2+} homeostasis is controlled principally by SERCA and the NCX, with minor contribution from the plasma membrane Ca^{2+}-ATPase. If FGF23 were increasing $[Ca^{2+}]i$ and the contraction by slowing Ca^{2+} removal, there should be a corresponding increase in τ (rate of relaxation following contraction). Our data show that FGF23 does not affect τ, demonstrating that it is unlikely to have a major acute effect on acute SERCA, NCX or Ca^{2+}-ATPase transporter function. Receptor antagonism with PD166866 was able to eliminate the changes in the contractile waveforms, demonstrating that FGFRs mediate the effects of FGF23 in the myocardium.

Significance

While an axis of signaling has been reported between bone and brain, gut, kidney, parathyroid, and adipose, potential endocrine crosstalk between bone and heart has not been well explored. A major question that arises from the current investigations on FGF23 and the heart: is FGF23 having both physiological and pathological effects on the myocardium? One possible physiological benefit of FGF23 altering cardiac contractility may be increasing renal phosphate clearance. Acutely increasing cardiac contractility may be a mechanism to increase cardiac output and increase renal blood flow. In addition, FGF23 may act on the heart to promote the expression of ANP/BNP which would increase vasodilation, natriuresis, and diuresis to clear excess phosphate. However, in CKD the increases in ANP/BNP are unable to improve renal clearance of phosphate. This accumulation of serum phosphate then elevates serum FGF23 which at high concentrations may promote cardiac dysfunction. This cycle appears to continue in CKD as increased ANP/BNP and FGF23 are predictive of CKD progression (10, 45) and cardiac pathologies (15, 21, 22, 26, 35, 43, 52).

From our findings we propose that FGF23 is behaving like other well characterized stress hormones (i.e.: norepinephrine, epinephrine, and angiotensin II). Acutely these hormones are inotropic and act to restore homeostasis; however, over the long-term chronic elevations in these hormones and $[Ca^{2+}]i$ can cause contractile dysfunction, remodeling of the heart, and progression to cardiac hypertrophy. Similarly, our findings have lead us to propose that endogenous FGF23 increases $[Ca^{2+}]i$ in cardiomyocytes. This finding is important as increases in $[Ca^{2+}]i$ can initially be diverted to the excitation-contraction coupling process and increased stimulation of CICR to improve cardiac contractility. However, long-term exposure to FGF23 may create disruptions in Ca^{2+} homeostasis that then activate transcriptional remodeling mechanisms which contribute to long-term impairments in contractile function and ultimately cardiac hypertrophy.

For example, it has been shown that FGF23 can activate the Ca^{2+} sensitive calcineurin-NFAT signaling pathway (13) suggesting that $[Ca^{2+}]i$ may be an important trigger for hypertrophic signaling in cardiomyoyctes. Thus, FGF23's induction of Ca^{2+} signals appears to be important for controlling both transcriptional regulation and contractility. Importantly, our data in the *Col4a3*$^{-/-}$ suggests that left ventricular dysfunction may precede the development of cardiac hypertrophy. This may have important implications on a patient's quality of life, and may also serve as an important clinical diagnostic marker for severity of disease.

In summary, our data show that FGF23 may have additional effects on the heart in addition to hypertrophy, specifically related to calcium handling and cardiac contractility. Therefore, our studies provide an important rationale to further investigate the mechanisms for direct effects of this important bone endocrine factor on the heart.

Disclosures

All authors state that they have no conflicts of interest.

Acknowledgments

We would like to thank Yixia Xie for her assistant in collecting histological data. This work was supported by NIH NIAMS GO Grant (1RC2AR058962) to LFB and MJW, R01 HL-089939 to BD, NIH NIDDK (K08-DK087949) to JRS, and an AHA SDG (11SDG5330016) to MJW.

References

1. **Ben-Dov IZ, Galitzer H, Lavi-Moshayoff V, Goetz R, Kuro-o M, Mohammadi M, Sirkis R, Naveh-Many T, and Silver J**. The parathyroid is a target organ for FGF23 in rats. *J Clin Invest* 117: 4003-4008, 2007.
2. **Bergwitz C, and Juppner H**. Regulation of phosphate homeostasis by PTH, vitamin D, and FGF23. *Annu Rev Med* 61: 91-104, 2010.
3. **Bers DM**. Calcium cycling and signaling in cardiac myocytes. *Annu Rev Physiol* 70: 23-49, 2008.
4. **Bonewald LF, and Wacker MJ**. FGF23 production by osteocytes. *Pediatric nephrology* 2012.
5. **Brunt KR, Tsuji MR, Lai JH, Kinobe RT, Durante W, Claycomb WC, Ward CA, and Melo LG**. Heme oxygenase-1 inhibits pro-oxidant induced hypertrophy in HL-1 cardiomyocytes. *Exp Biol Med (Maywood)* 234: 582-594, 2009.
6. **Chandrasekar B, Mummidi S, Claycomb WC, Mestril R, and Nemer M**. Interleukin-18 is a pro-hypertrophic cytokine that acts through a phosphatidylinositol 3-kinase-phosphoinositide-dependent kinase-1-Akt-GATA4 signaling pathway in cardiomyocytes. *J Biol Chem* 280: 4553-4567, 2005.
7. **Claycomb WC, Lanson NA, Jr., Stallworth BS, Egeland DB, Delcarpio JB, Bahinski A, and Izzo NJ, Jr.** HL-1 cells: a cardiac muscle cell line that contracts and retains phenotypic characteristics of the adult cardiomyocyte. *Proc Natl Acad Sci U S A* 95: 2979-2984, 1998.
8. **Dalal M, Sun K, Cappola AR, Ferrucci L, Crasto C, Fried LP, and Semba RD**. Relationship of serum fibroblast growth factor 23 with cardiovascular disease in older community-dwelling women. *Eur J Endocrinol* 165: 797-803, 2011.
9. **Dawn B, Guo Y, Rezazadeh A, Huang Y, Stein AB, Hunt G, Tiwari S, Varma J, Gu Y, Prabhu SD, Kajstura J, Anversa P, Ildstad ST, and Bolli R**. Postinfarct cytokine therapy regenerates cardiac tissue and improves left ventricular function. *Circ Res* 98: 1098-1105, 2006.
10. **Dieplinger B, Mueller T, Kollerits B, Struck J, Ritz E, von Eckardstein A, Haltmayer M, and Kronenberg F**. Pro-A-type natriuretic peptide and pro-adrenomedullin predict progression of chronic kidney disease: the MMKD Study. *Kidney Int* 75: 408-414, 2009.
11. **Eder P, and Molkentin JD**. TRPC channels as effectors of cardiac hypertrophy. *Circ Res* 108: 265-272, 2011.
12. **Ewald B, Ewald D, Thakkinstian A, and Attia J**. Meta-analysis of B type natriuretic peptide and N-terminal pro B natriuretic peptide in the diagnosis of clinical heart failure and population screening for left ventricular systolic dysfunction. *Intern Med J* 38: 101-113, 2008.
13. **Faul C, Amaral AP, Oskouei B, Hu MC, Sloan A, Isakova T, Gutierrez OM, Aguillon-Prada R, Lincoln J, Hare JM, Mundel P, Morales A, Scialla J, Fischer M, Soliman EZ, Chen J, Go AS, Rosas SE, Nessel L, Townsend RR, Feldman HI, St John Sutton M, Ojo A, Gadegbeku C, Di Marco GS, Reuter S, Kentrup D, Tiemann K, Brand M, Hill JA, Moe OW, Kuro OM, Kusek JW, Keane MG, and Wolf M**. FGF23 induces left ventricular hypertrophy. *J Clin Invest* 121: 4393-4408, 2011.
14. **Feng JQ, Ward LM, Liu S, Lu Y, Xie Y, Yuan B, Yu X, Rauch F, Davis SI, Zhang S, Rios H, Drezner MK, Quarles LD, Bonewald LF, and White KE**. Loss of DMP1 causes rickets and osteomalacia and identifies a role for osteocytes in mineral metabolism. *Nat Genet* 38: 1310-1315, 2006.
15. **Ford ML, Smith ER, Tomlinson LA, Chatterjee PK, Rajkumar C, and Holt SG**. FGF-23 and osteoprotegerin are independently associated with myocardial damage in chronic kidney disease stages 3 and 4. Another link between chronic kidney disease-mineral bone disorder and the heart. *Nephrol Dial Transplant* 27: 727-733, 2012.
16. **Goonasekera SA, and Molkentin JD**. Unraveling the secrets of a double life: contractile versus signaling Ca2+ in a cardiac myocyte. *J Mol Cell Cardiol* 52: 317-322, 2012.

17. **Gross O, Girgert R, Rubel D, Temme J, Theissen S, and Muller GA**. Renal protective effects of aliskiren beyond its antihypertensive property in a mouse model of progressive fibrosis. *Am J Hypertens* 24: 355-361, 2011.
18. **Gross O, Schulze-Lohoff E, Koepke ML, Beirowski B, Addicks K, Bloch W, Smyth N, and Weber M**. Antifibrotic, nephroprotective potential of ACE inhibitor vs AT1 antagonist in a murine model of renal fibrosis. *Nephrol Dial Transplant* 19: 1716-1723, 2004.
19. **Gruson D, Lepoutre T, Ketelslegers JM, Cumps J, Ahn SA, and Rousseau MF**. C-terminal FGF23 is a strong predictor of survival in systolic heart failure. *Peptides* 2012.
20. **Gutierrez OM, Januzzi JL, Isakova T, Laliberte K, Smith K, Collerone G, Sarwar A, Hoffmann U, Coglianese E, Christenson R, Wang TJ, deFilippi C, and Wolf M**. Fibroblast growth factor 23 and left ventricular hypertrophy in chronic kidney disease. *Circulation* 119: 2545-2552, 2009.
21. **Holden RM, Beseau D, Booth SL, Adams MA, Garland JS, Morton RA, Collier CP, and Foley RN**. FGF-23 is associated with cardiac troponin T and mortality in hemodialysis patients. *Hemodial Int* 16: 53-58, 2012.
22. **Hsu HJ, and Wu MS**. Fibroblast growth factor 23: a possible cause of left ventricular hypertrophy in hemodialysis patients. *Am J Med Sci* 337: 116-122, 2009.
23. **Hughes SE**. Differential expression of the fibroblast growth factor receptor (FGFR) multigene family in normal human adult tissues. *J Histochem Cytochem* 45: 1005-1019, 1997.
24. **Imanishi Y, Inaba M, Nakatsuka K, Nagasue K, Okuno S, Yoshihara A, Miura M, Miyauchi A, Kobayashi K, Miki T, Shoji T, Ishimura E, and Nishizawa Y**. FGF-23 in patients with end-stage renal disease on hemodialysis. *Kidney Int* 65: 1943-1946, 2004.
25. **Imel EA, Peacock M, Pitukcheewanont P, Heller HJ, Ward LM, Shulman D, Kassem M, Rackoff P, Zimering M, Dalkin A, Drobny E, Colussi G, Shaker JL, Hoogendoorn EH, Hui SL, and Econs MJ**. Sensitivity of fibroblast growth factor 23 measurements in tumor-induced osteomalacia. *J Clin Endocrinol Metab* 91: 2055-2061, 2006.
26. **Ix JH, Katz R, Kestenbaum BR, de Boer IH, Chonchol M, Mukamal KJ, Rifkin D, Siscovick DS, Sarnak MJ, and Shlipak MG**. Fibroblast growth factor-23 and death, heart failure, and cardiovascular events in community-living individuals: CHS (Cardiovascular Health Study). *J Am Coll Cardiol* 60: 200-207, 2012.
27. **Kabaeva Z, Zhao M, and Michele DE**. Blebbistatin extends culture life of adult mouse cardiac myocytes and allows efficient and stable transgene expression. *Am J Physiol Heart Circ Physiol* 294: H1667-1674, 2008.
28. **Kent RL, Rozich JD, McCollam PL, McDermott DE, Thacker UF, Menick DR, McDermott PJ, and Cooper Gt**. Rapid expression of the Na(+)-Ca2+ exchanger in response to cardiac pressure overload. *Am J Physiol* 265: H1024-1029, 1993.
29. **Kuro-o M, Matsumura Y, Aizawa H, Kawaguchi H, Suga T, Utsugi T, Ohyama Y, Kurabayashi M, Kaname T, Kume E, Iwasaki H, Iida A, Shiraki-Iida T, Nishikawa S, Nagai R, and Nabeshima YI**. Mutation of the mouse klotho gene leads to a syndrome resembling ageing. *Nature* 390: 45-51, 1997.
30. **Landstrom AP, Kellen CA, Dixit SS, van Oort RJ, Garbino A, Weisleder N, Ma J, Wehrens XH, and Ackerman MJ**. Junctophilin-2 expression silencing causes cardiocyte hypertrophy and abnormal intracellular calcium-handling. *Circ Heart Fail* 4: 214-223, 2011.
31. **Larsson T, Nisbeth U, Ljunggren O, Juppner H, and Jonsson KB**. Circulating concentration of FGF-23 increases as renal function declines in patients with chronic kidney disease, but does not change in response to variation in phosphate intake in healthy volunteers. *Kidney Int* 64: 2272-2279, 2003.
32. **Li H, Martin A, David V, and Quarles LD**. Compound deletion of Fgfr3 and Fgfr4 partially rescues the Hyp mouse phenotype. *Am J Physiol Endocrinol Metab* 300: E508-517, 2011.
33. **Lorenz K, Schmitt JP, Vidal M, and Lohse MJ**. Cardiac hypertrophy: targeting Raf/MEK/ERK1/2-signaling. *Int J Biochem Cell Biol* 41: 2351-2355, 2009.

34. **Mirza MA, Hansen T, Johansson L, Ahlstrom H, Larsson A, Lind L, and Larsson TE**. Relationship between circulating FGF23 and total body atherosclerosis in the community. *Nephrol Dial Transplant* 24: 3125-3131, 2009.
35. **Mirza MA, Larsson A, Melhus H, Lind L, and Larsson TE**. Serum intact FGF23 associate with left ventricular mass, hypertrophy and geometry in an elderly population. *Atherosclerosis* 207: 546-551, 2009.
36. **Negishi K, Kobayashi M, Ochiai I, Yamazaki Y, Hasegawa H, Yamashita T, Shimizu T, Kasama S, and Kurabayashi M**. Association between fibroblast growth factor 23 and left ventricular hypertrophy in maintenance hemodialysis patients. Comparison with B-type natriuretic peptide and cardiac troponin T. *Circ J* 74: 2734-2740, 2010.
37. **Panek RL, Lu GH, Dahring TK, Batley BL, Connolly C, Hamby JM, and Brown KJ**. In vitro biological characterization and antiangiogenic effects of PD 166866, a selective inhibitor of the FGF-1 receptor tyrosine kinase. *The Journal of pharmacology and experimental therapeutics* 286: 569-577, 1998.
38. **Pereira RC, Juppner H, Azucena-Serrano CE, Yadin O, Salusky IB, and Wesseling-Perry K**. Patterns of FGF-23, DMP1, and MEPE expression in patients with chronic kidney disease. *Bone* 45: 1161-1168, 2009.
39. **Plischke M, Neuhold S, Adlbrecht C, Bielesz B, Shayganfar S, Bieglmayer C, Szekeres T, Horl WH, Strunk G, Vavken P, Pacher R, and Hulsmann M**. Inorganic phosphate and FGF-23 predict outcome in stable systolic heart failure. *Eur J Clin Invest* 42: 649-656, 2012.
40. **Roos KP, Jordan MC, Fishbein MC, Ritter MR, Friedlander M, Chang HC, Rahgozar P, Han T, Garcia AJ, Maclellan WR, Ross RS, and Philipson KD**. Hypertrophy and heart failure in mice overexpressing the cardiac sodium-calcium exchanger. *J Card Fail* 13: 318-329, 2007.
41. **Sahn DJ, DeMaria A, Kisslo J, and Weyman A**. Recommendations regarding quantitation in M-mode echocardiography: results of a survey of echocardiographic measurements. *Circulation* 58: 1072-1083, 1978.
42. **Schiller NB, Shah PM, Crawford M, DeMaria A, Devereux R, Feigenbaum H, Gutgesell H, Reichek N, Sahn D, Schnittger I, and et al.** Recommendations for quantitation of the left ventricle by two-dimensional echocardiography. American Society of Echocardiography Committee on Standards, Subcommittee on Quantitation of Two-Dimensional Echocardiograms. *J Am Soc Echocardiogr* 2: 358-367, 1989.
43. **Seiler S, Cremers B, Rebling NM, Hornof F, Jeken J, Kersting S, Steimle C, Ege P, Fehrenz M, Rogacev KS, Scheller B, Bohm M, Fliser D, and Heine GH**. The phosphatonin fibroblast growth factor 23 links calcium-phosphate metabolism with left-ventricular dysfunction and atrial fibrillation. *Eur Heart J* 32: 2688-2696, 2011.
44. **Shalhoub V, Shatzen EM, Ward SC, Davis J, Stevens J, Bi V, Renshaw L, Hawkins N, Wang W, Chen C, Tsai MM, Cattley RC, Wronski TJ, Xia X, Li X, Henley C, Eschenberg M, and Richards WG**. FGF23 neutralization improves chronic kidney disease-associated hyperparathyroidism yet increases mortality. *J Clin Invest* 122: 2543-2553, 2012.
45. **Spanaus KS, Kronenberg F, Ritz E, Schlapbach R, Fliser D, Hersberger M, Kollerits B, Konig P, and von Eckardstein A**. B-type natriuretic peptide concentrations predict the progression of nondiabetic chronic kidney disease: the Mild-to-Moderate Kidney Disease Study. *Clin Chem* 53: 1264-1272, 2007.
46. **Stubbs JR, He N, Idiculla A, Gillihan R, Liu S, David V, Hong Y, and Quarles LD**. Longitudinal evaluation of FGF23 changes and mineral metabolism abnormalities in a mouse model of chronic kidney disease. *Journal of bone and mineral research : the official journal of the American Society for Bone and Mineral Research* 2011.
47. **Takeshita K, Fujimori T, Kurotaki Y, Honjo H, Tsujikawa H, Yasui K, Lee JK, Kamiya K, Kitaichi K, Yamamoto K, Ito M, Kondo T, Iino S, Inden Y, Hirai M, Murohara T, Kodama I, and Nabeshima Y**.

Sinoatrial node dysfunction and early unexpected death of mice with a defect of klotho gene expression. *Circulation* 109: 1776-1782, 2004.

48. **Taylor EN, Rimm EB, Stampfer MJ, and Curhan GC**. Plasma fibroblast growth factor 23, parathyroid hormone, phosphorus, and risk of coronary heart disease. *Am Heart J* 161: 956-962, 2011.

49. **Teichholz LE, Kreulen T, Herman MV, and Gorlin R**. Problems in echocardiographic volume determinations: echocardiographic-angiographic correlations in the presence of absence of asynergy. *Am J Cardiol* 37: 7-11, 1976.

50. **Touchberry CD, Bales IK, Stone JK, Rohrberg TJ, Parelkar NK, Nguyen T, Fuentes O, Liu X, Qu CK, Andresen JJ, Valdivia HH, Brotto M, and Wacker MJ**. Phosphatidylinositol 3,5-bisphosphate (PI(3,5)P2) potentiates cardiac contractility via activation of the ryanodine receptor. *J Biol Chem* 285: 40312-40321, 2010.

51. **Touchberry CD, Elmore CJ, Nguyen TM, Andresen JJ, Zhao X, Orange M, Weisleder N, Brotto M, Claycomb WC, and Wacker MJ**. Store-operated calcium entry is present in HL-1 cardiomyocytes and contributes to resting calcium. *Biochem Biophys Res Commun* 416: 45-50, 2011.

52. **Unsal A, Kose Budak S, Koc Y, Basturk T, Sakaci T, Ahbap E, and Sinangil A**. Relationship of Fibroblast Growth Factor 23 with Left Ventricle Mass Index and Coronary Calcificaton in Chronic Renal Disease. *Kidney Blood Press Res* 36: 55-64, 2012.

53. **Urakawa I, Yamazaki Y, Shimada T, Iijima K, Hasegawa H, Okawa K, Fujita T, Fukumoto S, and Yamashita T**. Klotho converts canonical FGF receptor into a specific receptor for FGF23. *Nature* 444: 770-774, 2006.

54. **Wacker MJ, and Godard MP**. Analysis of one-step and two-step real-time RT-PCR using SuperScript III. *Journal of biomolecular techniques : JBT* 16: 266-271, 2005.

55. **Wacker MJ, and Godard MP**. Analysis of one-step and two-step real-time RT-PCR using SuperScript III. *J Biomol Tech* 16: 266-271, 2005.

56. **Wacker MJ, Kosloski LM, Gilbert WJ, Touchberry CD, Moore DS, Kelly JK, Brotto M, and Orr JA**. Inhibition of thromboxane A2-induced arrhythmias and intracellular calcium changes in cardiac myocytes by blockade of the inositol trisphosphate pathway. *J Pharmacol Exp Ther* 331: 917-924, 2009.

57. **Wacker MJ, Kosloski LM, Gilbert WJ, Touchberry CD, Moore DS, Kelly JK, Brotto M, and Orr JA**. Inhibition of thromboxane A2-induced arrhythmias and intracellular calcium changes in cardiac myocytes by blockade of the inositol trisphosphate pathway. *The Journal of pharmacology and experimental therapeutics* 331: 917-924, 2009.

58. **Yamazaki M, Ozono K, Okada T, Tachikawa K, Kondou H, Ohata Y, and Michigami T**. Both FGF23 and extracellular phosphate activate Raf/MEK/ERK pathway via FGF receptors in HEK293 cells. *J Cell Biochem* 111: 1210-1221, 2010.

59. **Yu X, Ibrahimi OA, Goetz R, Zhang F, Davis SI, Garringer HJ, Linhardt RJ, Ornitz DM, Mohammadi M, and White KE**. Analysis of the biochemical mechanisms for the endocrine actions of fibroblast growth factor-23. *Endocrinology* 146: 4647-4656, 2005.

60. **Zhang X, Ibrahimi OA, Olsen SK, Umemori H, Mohammadi M, and Ornitz DM**. Receptor specificity of the fibroblast growth factor family. The complete mammalian FGF family. *J Biol Chem* 281: 15694-15700, 2006.

61. **Zuba-Surma EK, Guo Y, Taher H, Sanganalmath SK, Hunt G, Vincent RJ, Kucia M, Abdel-Latif A, Tang XL, Ratajczak MZ, Dawn B, and Bolli R**. Transplantation of expanded bone marrow-derived very small embryonic-like stem cells (VSEL-SCs) improves left ventricular function and remodelling after myocardial infarction. *J Cell Mol Med* 15: 1319-1328, 2011.

Figure Legends

Fig. 1: FGF23 increases cell size in a dose dependent manner. ***A*** Representative forward-scatter histograms (FSC-H) of HL-1 cardiomyocytes treated with vehicle or FGF23 (900 pg/ml) for 48 h; T(X)=63. ***B*** Summary of forward-scatter (FSC-H) data on cardiomyocytes treated with increasing doses of FGF23 (9-900 pg/ml) using flow cyctometry (T(X)=63, $p<0.01$). FSC-H analysis of >10,000 live gated cells per sample (n= 5 experiments). Results from independent experiments were normalized to vehicle controls, and averaged. *denotes statistical significance from vehicle. † denotes statistical difference from FGF23 (9 pg/ml) treatment.

Fig. 2: FGF23 increases markers of hypertrophy in mouse ventricular tissue via FGFR. ***A*** FGF23 exposure increased the early response gene EGR1 and the hypertrophy associated genes ANP and BNP after 24 h. Forty-eight h treatment with FGF23 increased the expression of other hypertrophy genes βMHC and SkAct (n=7). ***B*** FGF23 treatment increased ERK phosphorylation after 15 min (n=4). ***C*** Total protein content of ventricular muscle strips increased following 48 h treatment with FGF23 and was blocked by pre-treatment with PD166866 (n=5-7). *denotes statistical significance from vehicle.

Fig. 3: FGFRs and *α-Klotho* are expressed in isolated adult ventricular cardiomyocytes. ***A*** Real-time RT-PCR reaction (run in triplicates) showing the average fluorescence values at each cycle number for FGFR1-4 and *α-Klotho* from isolated adult ventricular cardiomyocytes. ***B*** Summary of the relative expression data from cardiomyocytes for FGFRs when normalized to the lowest expressed gene (*α-Klotho*) (n=6). Statistics were conducted on the non-normalized gene expression data and are reported in the results.

Fig. 4: *Col4a3*$^{-/-}$ mouse hearts express genetic markers of hypertrophy but do not display increases in gross or cellular measures of hypertrophy. ***A*** Hearts from 10 week old *Col4a3*$^{-/-}$ mice had increased expression of the hypertrophy associated genes ANP, βMHC and SkAct (n=6). ***B*** *Col4a3*$^{-/-}$ mice did not show any changes in anterior (Ant.) or posterior (Pst.) wall thickness during diastole obtained by echocardiography (n=12-13). ***C*** No changes were observed in the left ventricular (LV) mass/body weight (BW) ratio (mg/g), nor when heart weight (HW) was compared to tibia length (TL) in the *Col4a3*$^{-/-}$ mice (n=12-13). ***D*** Representative images showing WGA stained cardiomyocytes sectioned from *Col4a3*$^{-/-}$ and WT mouse hearts. ***E*** Summary of cardiomyocyte cross-sectional area data from WT and *Col4a3*$^{-/-}$ cardiomyocytes (n=3 animals/group). *denotes statistical significance from vehicle.

Fig. 5: *Col4a3*$^{-/-}$ mice hearts display reduced left ventricular function. ***A*** Representative M-Mode images showing reduced systolic excursion of LV walls in *Col4a3*$^{-/-}$ mice (bottom panel), indicating reduced systolic function compared with their WT littermates (top panel). ***B*** Quantitative echocardiographic data show reduced LV function as evidenced by lower fractional shortening (FS) and ejection fraction (EF) in *Col4a3*$^{-/-}$ mice compared with WT littermates. *denotes statistical significance from WT.

Fig. 6: FGF23 treatment increases [Ca^{2+}]*i* in primary cardiomyocytes. ***A*** Acute fluo-4 changes in [Ca^{2+}]*i* (in relative fluorescent units, R.F.U) in primary cardiomyocytes immediately following treatment with FGF23, in the presence of extracellular Ca^{2+}. For the fluorescent images, warmer colors (yellows/reds) indicated increased fluorescence (increase in [Ca^{2+}]*i*). ***B***

Fluo-4 image of a primary cardiomyocyte at baseline and at the peak fluorometric response following acute FGF23 treatment. ***C*** Summary data showing the average acute changes in fluorescence mediated by FGF23 and during receptor antagonism (PD166866) (n=10-30 cells; 3-5 animals). Measurements are indicated as a change in fluorescence after treatment divided by the initial fluorescence (F/F_O). ***D*** Summary data showing the average changes in fluorescence mediated by FGF23, FGF23 treatment in the absence of extracellular Ca^{2+} (0 mM; +0 Ca^{2+}), and following pre-treatment with verapamil (Verap) (n=10-30 cells; 3-5 animals). *denotes statistical significance from vehicle. † denotes statistical difference from FGF23 treatment.

Fig. 7: FGF23 acutely increases contractile force in *ex vivo* ventricular muscle strips via FGFR. ***A*** Tracings of left ventricular muscle contractions at baseline and following treatment with either FGF23 or vehicle. ***B*** Mean changes in isometric tension data induced by FGF23 or vehicle normalized to baseline contractions. ***C*** FGF23 treatment increased the slope and area of the contractile waveforms, but not the rate of relxation, τ (n=6-12 animals). ***D*** PD166866 pre-treatment prevents FGF23 induced increases in tension, slope and area. No changes were noted in τ as a result of FGF23, PD166866 or vehicle treatments (n=6-12). *denotes statistical significance from vehicle. †denotes statistical difference from FGF23 treatment.

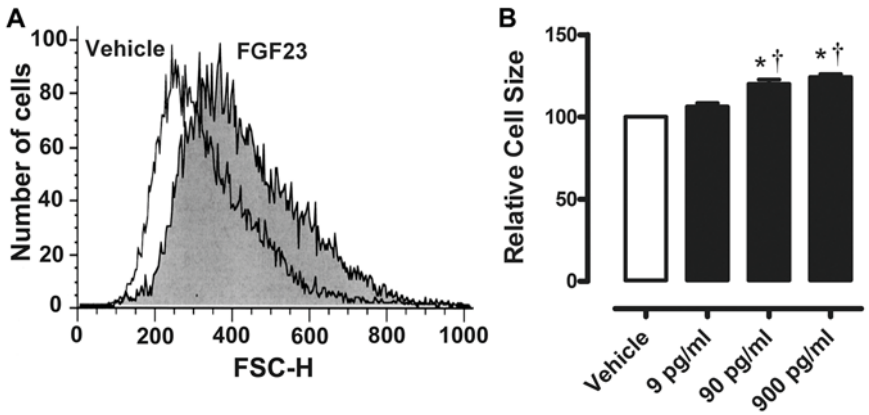
A
Vehicle
FGF23
Number of cells
100
80
60
40
20
0
0
200
400
600
800
1000
FSC-H
B
Relative Cell Size
150
100
50
0
*†
*†
Vehicle
9 pg/ml
90 pg/ml
900 pg/ml

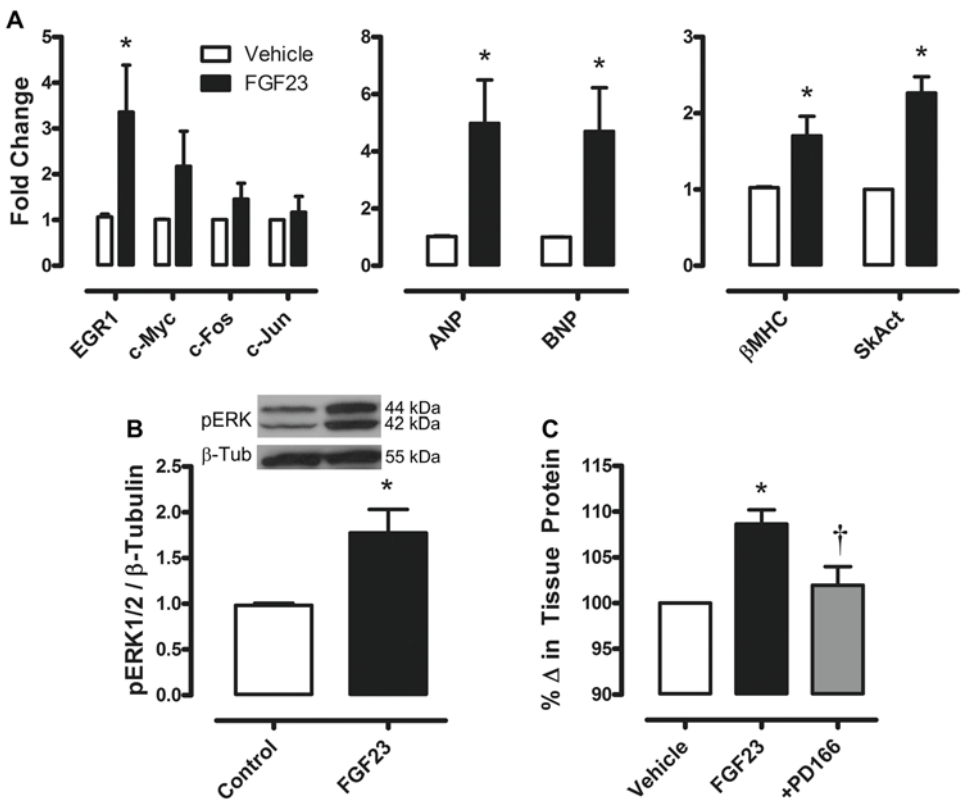
A
Fold Change
Vehicle
FGF23
EGR1
c-Myc
c-Fos
c-Jun
ANP
BNP
βMHC
SkAct
B
pERK
β-Tub
44 kDa
42 kDa
55 kDa
pERK1/2 / β-Tubulin
Control
FGF23
C
% Δ in Tissue Protein
Vehicle
FGF23
+PD166

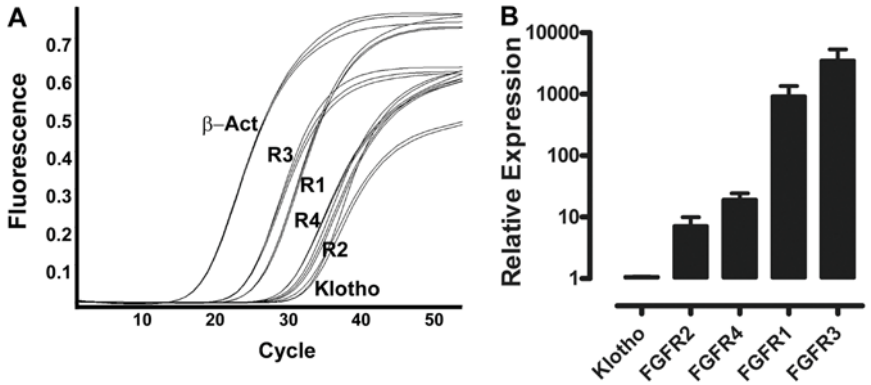
A
Fluorescence
0.7
0.6
0.5
0.4
0.3
0.2
0.1
β–Act
R3
R1
R4
R2
Klotho
10
20
30
40
50
Cycle
B
Relative Expression
10000
1000
100
10
1
Klotho
FGFR2
FGFR4
FGFR1
FGFR3

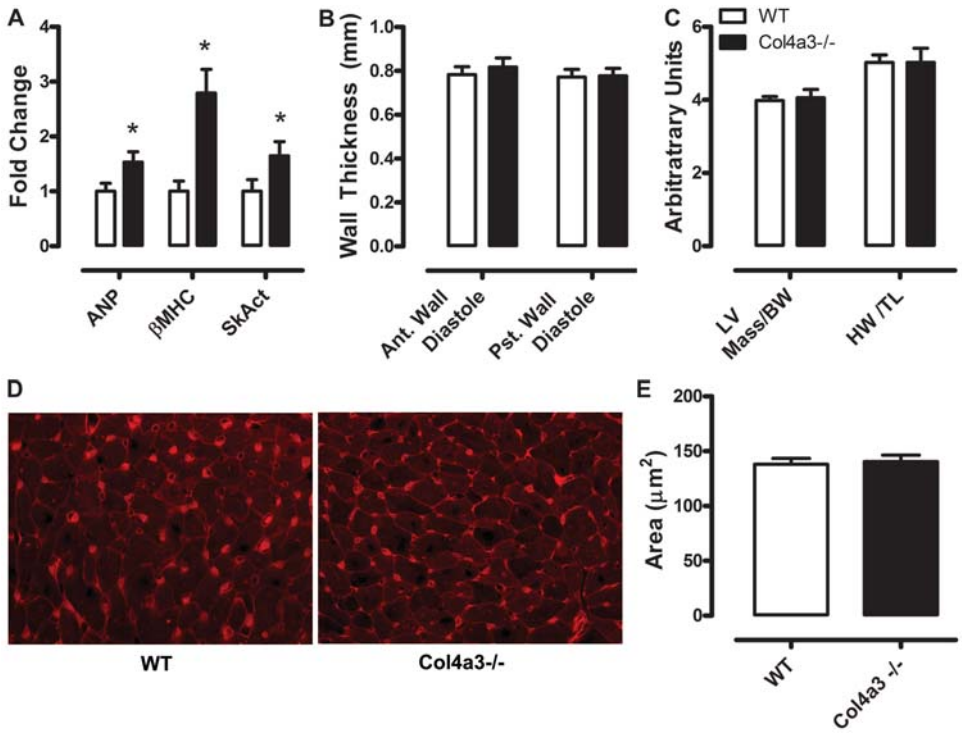
A
Fold Change
0
1
2
3
4
*
*
*
ANP
βMHC
SkAct
B
Wall Thickness (mm)
0.0
0.2
0.4
0.6
0.8
1.0
Ant. Wall Diastole
Pst. Wall Diastole
C
WT
Col4a3-/-
Arbitratrary Units
0
2
4
6
LV Mass/BW
HW /TL
D
WT
Col4a3-/-
E
Area (μm2)
0
50
100
150
200
WT
Col4a3 -/-

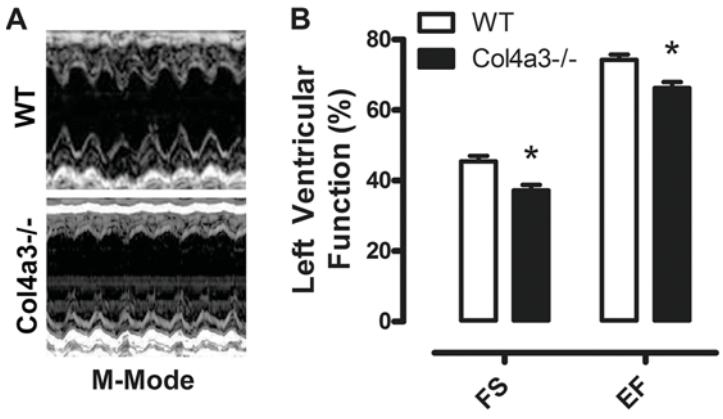
A
WT
Col4a3-/-
M-Mode
B
WT
Col4a3-/-
Left Ventricular Function (%)
80
60
40
20
0
*
*
FS
EF

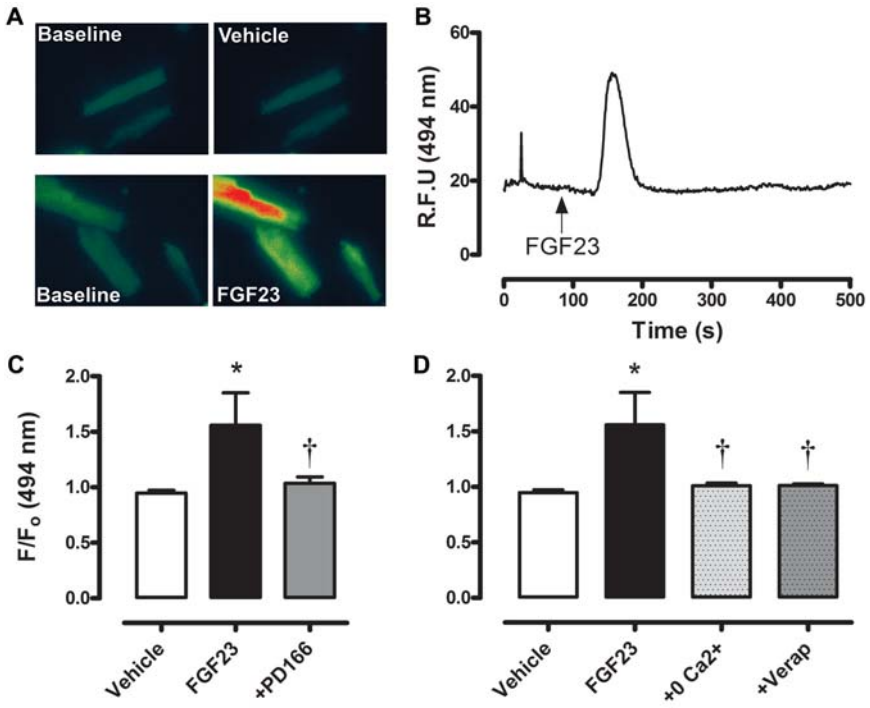
A
Baseline
Vehicle
Baseline
FGF23
B
R.F.U (494 nm)
60
40
20
0
FGF23
0
100
200
300
400
500
Time (s)
C
F/Fo (494 nm)
2.0
1.5
1.0
0.5
0.0
*
†
Vehicle
FGF23
+PD166
D
2.0
1.5
1.0
0.5
0.0
*
†
†
Vehicle
FGF23
+0 Ca2+
+Verap

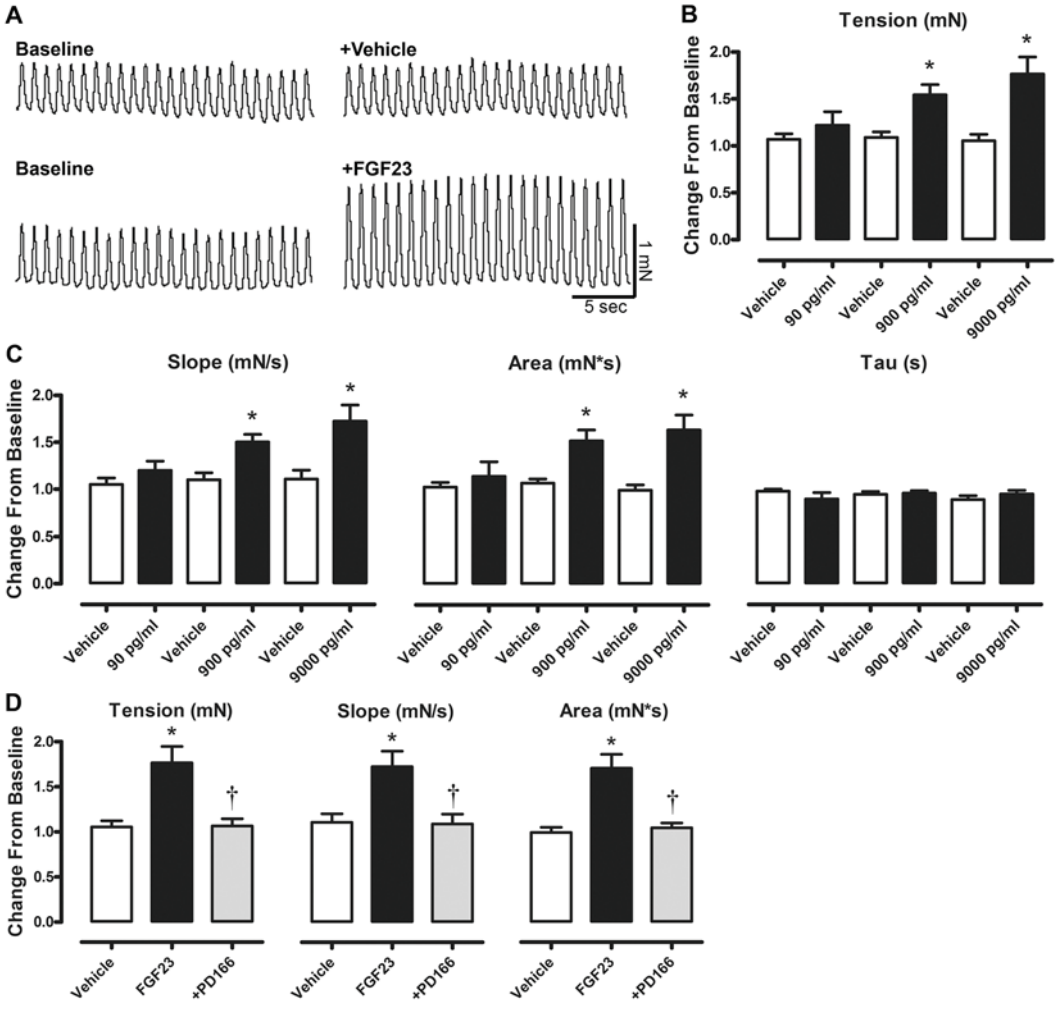
A
Baseline
+Vehicle
Baseline
+FGF23
1 mN
5 sec
B
Tension (mN)
Change From Baseline
2.0
1.5
1.0
0.5
0.0
*
*
Vehicle
90 pg/ml
Vehicle
900 pg/ml
Vehicle
9000 pg/ml
C
Slope (mN/s)
Area (mN*s)
Tau (s)
Change From Baseline
2.0
1.5
1.0
0.5
0.0
*
*
*
*
Vehicle
90 pg/ml
Vehicle
900 pg/ml
Vehicle
9000 pg/ml
D
Tension (mN)
Slope (mN/s)
Area (mN*s)
Change From Baseline
2.0
1.5
1.0
0.5
0.0
*
*
*
†
†
†
Vehicle
FGF23
+PD166